16th World Conference on Earthquake, 16WCEE 2017

Santiago Chile, January 9th to 13th 2017

Paper N° 4648

Registration Code: S-E1462972000

SEISMIC WAVE AMPLIFICATION IN 3D ALLUVIAL BASINS: AGGRAVATION FACTORS FROM FAST MULTIPOLE BEM SIMULATIONS

K.C. Meza-Fajardo[(1)], J.F. Semblat[(2)], S. Chaillat [(3)], L. Lenti[(4)]

[(1)] *Research Engineer, BRGM, Risk and Prevention Division, Seismic and Volcanic Risk Unit, 45060 Orléans Cedex 2, France* *k.mezafajardo@brgm.fr*

[(2)] *Head, Université Paris-Est, IFSTTAR, Dépt GERS, Laboratoire Séismes et Vibrations, F-77447 Marne la Vallée Cedex 2, France,* *jean-francois.semblat@ifsttar.fr*

[(3)] *Researcher, Laboratoire Poems (UMR 7231 CNRS-INRIA-ENSTA), 91762 Palaiseau Cedex, France,* *stephanie.chaillat@ensta-paristech.fr*

[(4)] *Researcher, Université Paris-Est, IFSTTAR, Dépt GERS, Laboratoire Séismes et Vibrations, F-77447 Marne la Vallée Cedex 2, France,* *luca.lenti@ifsttar.fr*

Abstract

In this work, we study seismic wave amplification in alluvial basins having 3D canonical geometries through the Fast Multipole Boundary Element Method in the frequency domain. We investigate how much 3D amplification differs from the 1D (horizontal layering) and the 2D cases. Considering synthetic incident wave-fields, we examine the relationships between the amplification level and the most relevant physical parameters of the problem (impedance contrast, 3D aspect ratio, vertical and oblique incidence of plane waves). The FMBEM results show that the most important parameters for wave amplification are the impedance contrast and equivalent shape ratio. Using these two parameters, we derive simple rules to compute the fundamental frequency for different 3D basin shapes and the corresponding 3D aggravation factor for 5% damping. Effects on amplification due to 3D basin asymmetry are also studied and incorporated in the derived rules..

Keywords: site effects, wave amplification, aggravation factors, 3D effects, numerical modelling

1. Introduction

Seismic wave amplification is an important aspect in seismic hazard assessment, as it is a crucial step to determine the seismic demands for any engineering project. Seismic codes commonly require its estimation by means of simplified 1D models of the geological setting of the site of interest. However, wave amplification in a basin is not only a result of changes in its mechanical properties, but also a consequence of its geometry: constructive interference, trapping of waves and generation of surface waves at basin edges (e.g., [1]). The influence of geometry in wave amplification cannot be reproduced with 1D models and thus these models lead to responses much lower than those obtained with 2D/3D models. In this work we estimate amplification of incident plane waves in alluvial basins with simple, 3D standard geometries, and compare it with amplification based on 1D models. Similar problems have been investigated by other authors in the past considering simple basin geometries. In [2] Rodriguez-Zuñiga *et al*. studied the case of a 3D cylindrical basin having a rectangular vertical cross-section and found a large difference between the 2D and 3D response at the center of the basin. Papageorgiou and Pei [3] considered incident body and Rayleigh waves in 3D cylindrical basins with semicircular cross-section. Bard and Bouchon in [4] and Jiang and Kuribayashi in [5] reported that the fundamental frequencies of the basins only depend on the aspect ratio and the 1D fundamental frequency at the center of the valley. Smerzini *et al*. in [6] made comparisons of 3D, 2D and 1D amplification using the Spectral Element Method with a 3D model of the Gubbio plain in Italy. Olsen *et al*. in [7] found differences among 3D/2.5D/1D amplification and duration with a 3D finite difference model of the Upper Borrego Valley, California.

Since in the present study we consider basins completely embedded in a halfspace, we perform numerical simulations exploiting the efficiency of the Fast Multipole Boundary Element Method (FMBEM) for viscoelastic media [8]. Following the ideas for 2D canonical models presented by Makra *et al*. in [9] and Semblat *et al*. in [10], we synthesize the results to propose simple rules for 3D/1D amplification factors including 3D basin asymmetry effects.

2. Numerical model for basin geometry

Our first FMBEM model consists of a semi-spherical basin embedded in a halfspace as shown in Figure 1. The mesh includes the free surface because our FMBEM model is formulated in terms of the full-space fundamental solution. An incident field of plane *S*-waves is used as the input motion for our simulations. The relationship between the depth of the basin *h* and its radius *R* follows the equation:

$$\left(\frac{x}{R}\right)^2+\left(\frac{y}{R}\right)^2+\left(\frac{z}{h}\right)^2=1, \qquad z\leq 0 \tag{1}$$

where *x*, *y* and *z* are the space coordinates of the 3D basin. The parameters defining the geometrical and mechanical properties are listed in Table 1, where properties with subscript 2 correspond to the basin, and properties with subscript 1 correspond to the half-space.

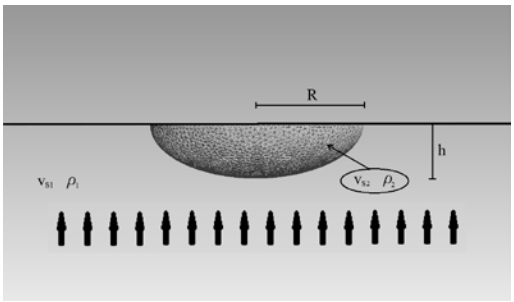

Figure 1. A 3D semi-spherical basin embedded in a half space and subjected to a plane wavefield. The horizontal and vertical components of the basin displacement are computed at the top (free) surface.

Table 1. Mechanical properties for basin and half-space.

Parameter	Value
Maximum depth (h)	1
Aspect ratio (k_h=R/h)	R
Radius of half space	5R
S-wave velocities ratio (χ)	v_{s2}/v_{s1}
Ratio of densities (ρ_2/ρ_1)	0.6
Poisson ratio of basin (ν_2)	0.30
Poisson ratio of half-space (ν_1)	0.25
Damping ratio of basin (ξ_2)	5%
Damping ratio of half-space (ξ_1)	0.5%

The second basin shape we consider in this study is a super-ellipsoid of degree five, which gives the basin a box shape, as shown in Figure 2a. The equation describing this shape is the following:

$$\left|\frac{x}{R}\right|^5 + \left|\frac{y}{R}\right|^5 + \left|\frac{z}{h}\right|^5 = 1, \qquad z \le 0 \tag{2}$$

where the symbol $|\cdot|$ denotes the absolute value of its argument. A basin cosine shape was also studied, defined in 3D by the expressions:

$$4p^2\left(\frac{z}{h}\right) = \left[\cos\left(\pi s\frac{x}{R}\right) + 2p - 1\right]\left[\cos\left(\pi s\frac{y}{R}\right) + 2p - 1\right]$$
$$\cos(\pi s) = 1 - 2p \tag{3}$$

Here the parameter p defines the percentage of the height of a full cosine cycle, that is, the total depth of the basin is 1, but the shape is scaled such that its height is only p of the total height of a full cosine cycle. In Figure 2a, the basin cosine shape is defined with p = 0.9, to avoid numerical artifacts at the intersection of the basin boundary and the free surface. The three different basin shapes shown in Figure 2a have the same shape ratio R/h, so we use the "equivalent shape ratio" l_o/h (as defined in [5]) to take into account the difference in thickness of the three basin shapes. The length l_o is the half width over which the depth of the basin is half its maximum value, as shown in Figure 2a.

(a) (b)

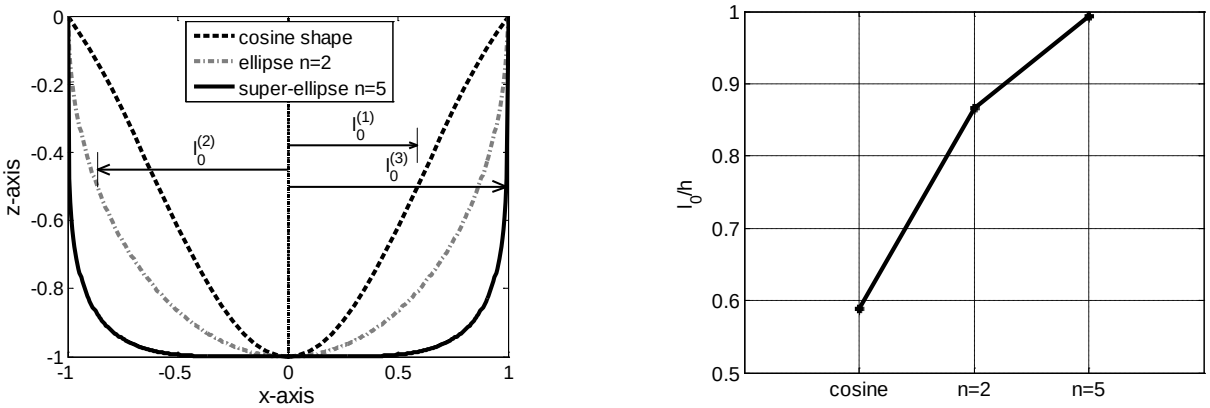

Figure 2. Three basin shapes considered in the study. (a) *x*-*z* cross section (b) Equivalent shape ratio l_o/h for the three basin shapes with a unitary radius.

3. 3D amplification due to incident *S*-waves

3.1 Semi-spherical basin

Incident *S*-waves polarized in the *x*-direction impinging on the basin will result in amplification of two components of displacement; therefore we define amplification factors for them in terms of magnitude of the free-field displacement U^F as follows:

$$A_V = \frac{\max(U_z^B)}{\max(U^F)}, \qquad A_H = \frac{\max(U_H^B)}{\max(U^F)} \tag{4}$$

where A_H and A_V are the amplification factors for the horizontal and vertical displacement components respectively. The parameters $U_Z{}^B$ and $U_H{}^B$ are the magnitudes of the horizontal and vertical components of displacement at the top of the basin, respectively. Figure 3 illustrates amplification factors for *S*-waves with incidence angles θ = 0°, 30° and 45° for deep basins (*R/h*=0.5, *R/h*=1). The amplification factors A_H and $-A_V$, are plotted in the same axis to illustrate their variation with frequency, keeping in mind that A_V is always positive. The results are presented in terms of a normalized frequency f / f_{rs}, where $f_{rs} = v_{s2}/4h$.

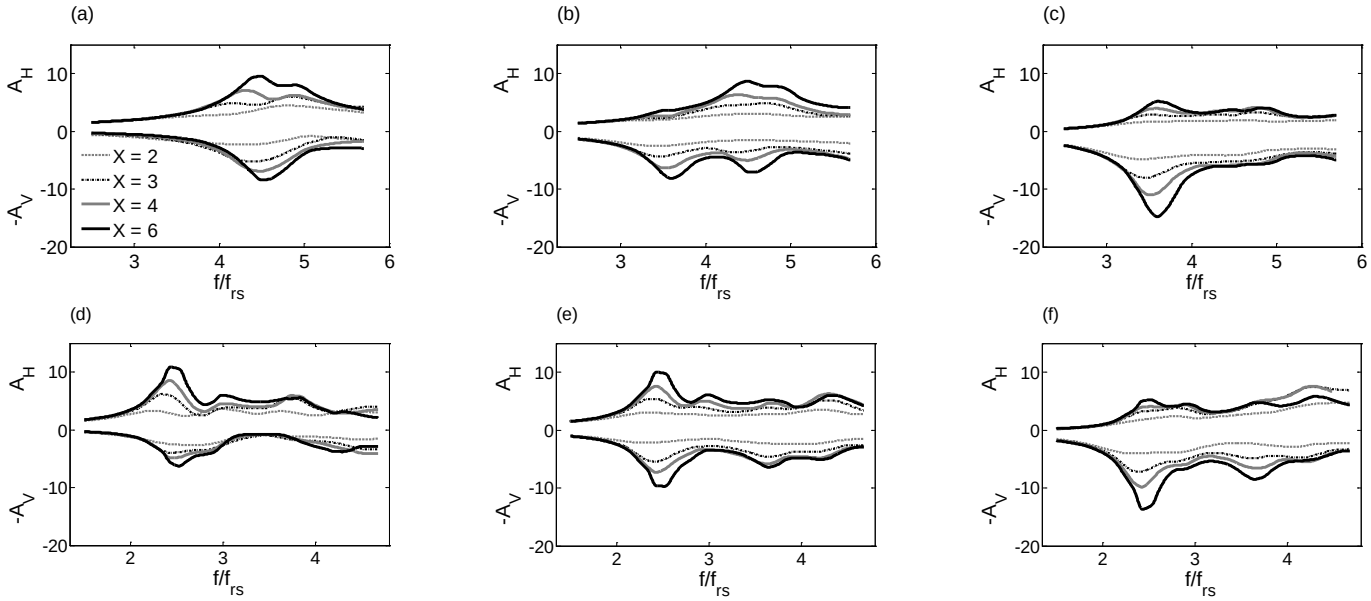

Figure 3. Comparison of amplification at the top of the 3D basin due to *S*-waves with different angles of incidence. (a) *R/h*=0.5, θ = 0°, (b) *R/h*=0.5, θ = 30°, (c) *R/h*=0.5, θ = 45° (d) *R/h*=1, θ = 0°, (e) *R/h*=1, θ = 30°, (f) *R/h*=1, θ = 45°.

From Figure 3 we can make the following observations:

(a) The fundamental frequency is mainly determined by the aspect ratio, and it is practically independent of the ratio of velocities,

(b) As the angle of incidence increases, the amplification of the horizontal component is reduced, whereas the amplification of the vertical component is increased.

(c) Surface waves may contribute to the higher amplification in the vertical component when θ = 45°.

3.2 Influence of basin "thickness"

In Figure 4 we show the obtained amplification factors for basins with the same aspect ratio *R/h* but with different equivalent aspect ratio l_o/h. For these analyses the input motion is given by vertically incident *S*-waves. Two aspect ratios were considered, k_h = 0.5 (Figures 4a-4c), and k_h = 2 (Figures 4d-4f). As Figure 4 indicates, the thickness of the basin has little influence on the amplification factors. However, a slightly higher amplification can be observed for the basin with lowest thickness (the cosine shape), probably due to strong basin edge effects and more pronounced trapping of waves. Furthermore, for the two considered aspect ratios the normalized fundamental frequency f/f_{rs} has little variation with the velocity ratio (below 25% for k_h = 0.5 and about 7% for k_h = 2). On the other hand, the equivalent aspect ratio l_o/h makes a significant difference on the fundamental and dominant (second mode) frequencies. For the basin with aspect ratio k_h = 0.5 the maximum variation of f/f_{rs} with l_o/h is of 44%. In the case of the normalized predominant frequency f/f_{ps}, the maximum variation is about 45%.

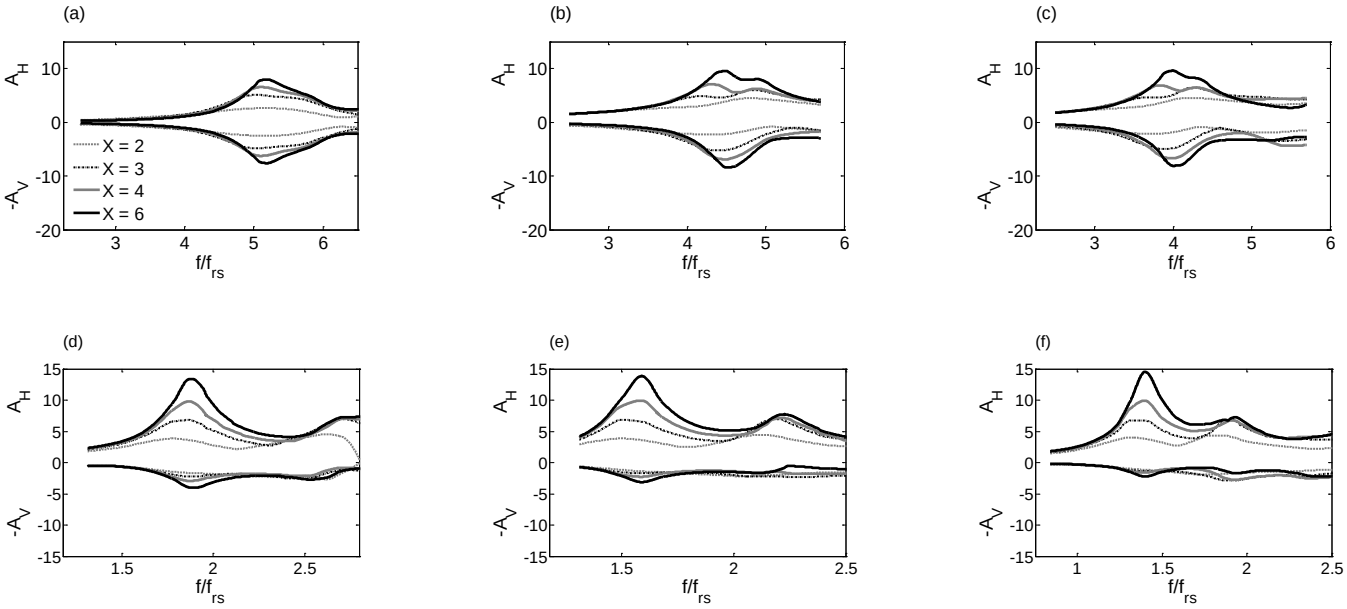

Figure 4. Amplification at the top of the 3D basin due to vertically incident *S*-waves with different equivalent shape ratios. (a) *R/h* = 0.5, basin with cosine shape (b) *R/h* = 0.5, basin with ellipsoidal shape, *n* = 2 (c) *R/h* = 0.5, basin with super-ellipsoidal shape, *n* = 5 (d) *R/h* = 2, basin with cosine shape (e) *R/h* = 2, basin with ellipsoidal shape, *n* = 2 (f) *R/h* = 2, basin with super-ellipsoidal shape, *n* = 5.

3.2 Effects of Asymmetry

When the basin has asymmetry with respect to one of the horizontal dimensions, wave amplification due to a vertically incident *S*-wave will be expected to be different when compared to the results presented in previous sections. To assess the effects of basin asymmetry, we change the radius of the basin in the *x*- or *y*- directions. For the basin of Figure 5a the radius in the *y*- direction R_y is the double of the radius in the *x*-direction R_x, whereas for the basin of Figure 5b the radius in the *x*-direction R_x is twice the radius in the *y*-direction R_y. The effect of asymmetry will then be different for these two cases since the dimension of lower basin thickness would be either parallel or perpendicular to the direction of polarization of the incident *S*-wave. As a third case we consider vertically incident *S*-waves polarized with 45° angle from the *x*- axis, as shown in Figure 5c.

In Figure 6 we can see the amplification factor for the symmetric, and the two asymmetric basins, with aspect ratios along the *x*-axis k_h=3. We obtain similar results for the symmetric basin and the asymmetric basin with R_x/R_y = 2, we believe because these two basins have the same radius R_x which is parallel to the direction

the *S*-wave is polarized. The other asymmetric basin (with R_x/R_y = 0.5) has a smaller R_x, and thus we obtain lower amplification levels, although Figure 6 shows the difference is not significant. Figure 6(d) shows that when the direction of polarization is 45° from the *x*-axis the amplification is reduced. From the results we conclude that the main effect of basin asymmetry is an increase in the fundamental and predominant frequencies, whereas amplification levels are increased (for the case R_x/R_y = 2) only about 10% with respect to symmetric basins.

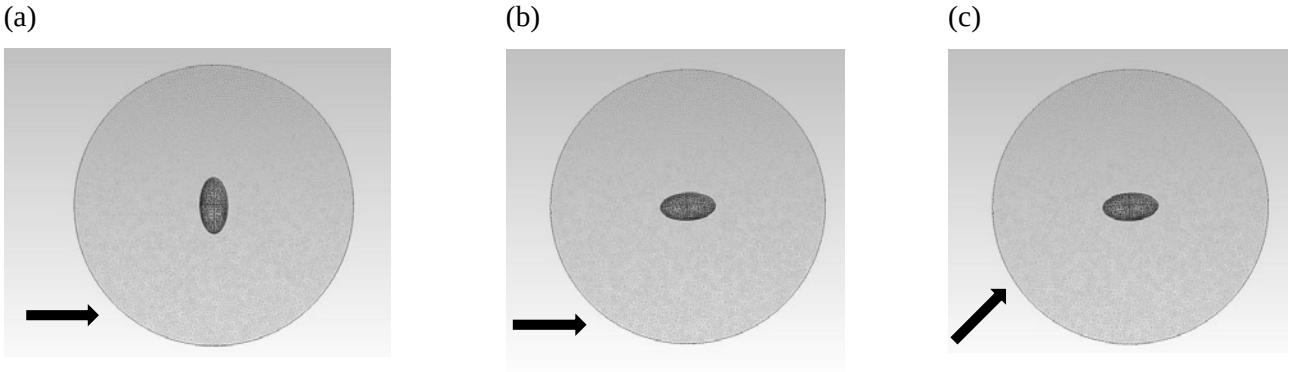

Figure 5. 3D basin models with asymmetry. (a) Basin with R_x/R_y = 0.5, (b) Basin with R_x/R_y = 2, (c) Basin with R_x/R_y = 2, direction of polarization of incident plane wave 45°.

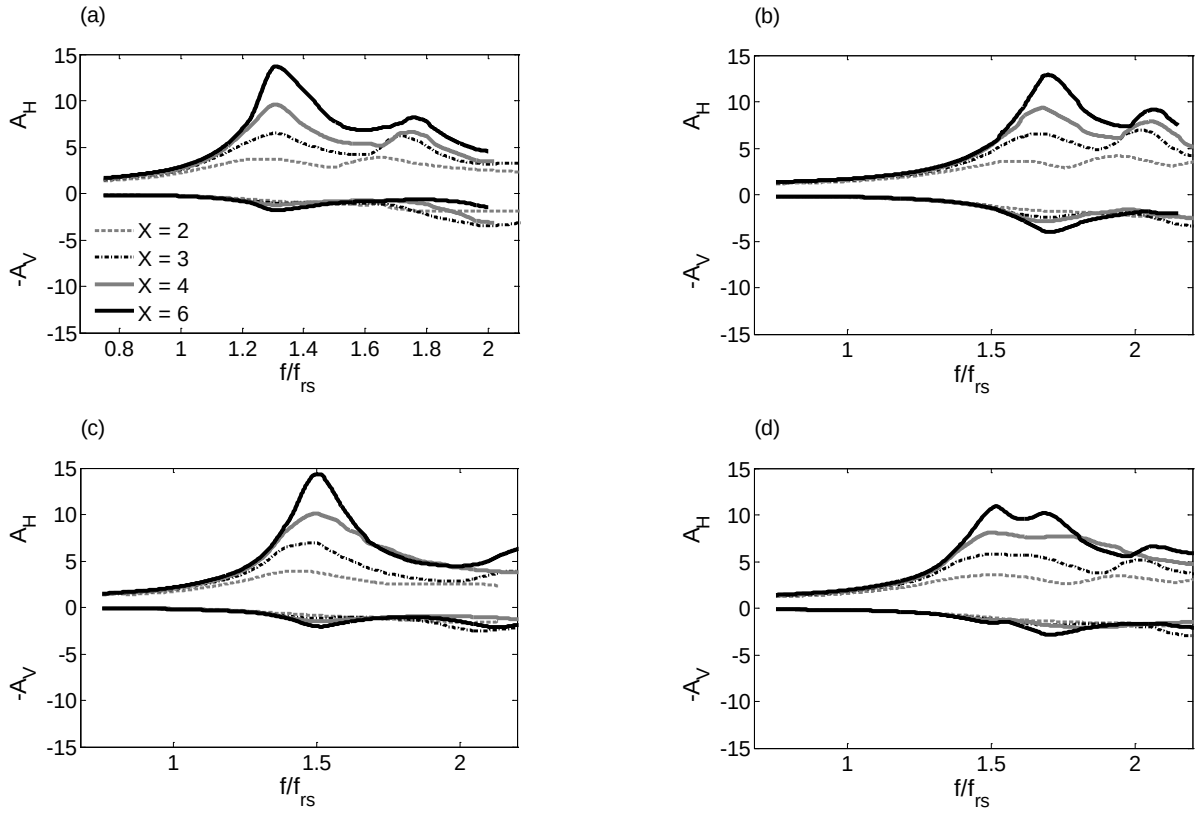

Figure 6. Amplification at the top of the 3D basin due to vertically incident *S*-waves for k_h = 3. (a) Symmetric basin (b) Basin with R_x/R_y = 0.5, (c) Basin with R_x/R_y =2, (d) Basin with R_x/R_y =2, and polarization direction at 45° with respect to the *x*-axis.

4. Simple Rules to Assess 3D Basin Effects

Considering the analyses with simple models presented in the previous sections, we propose rules to compute 3D/1D amplifications factors and their corresponding fundamental frequencies. These rules may allow engineers and analysts to estimate amplification considering 3D effects without performing complex numerical 3D simulations. However, since we are considering only the fundamental mode of basin vibration, it should be understood the amplification factor for *S*-waves estimated by the rules corresponds to the center of the basin. In Figure 7 we present the plot of the proposed rules, and the data used to construct them. For the normalized fundamental frequency of the basin, we propose the following equation, given in terms of the equivalent shape ratio l_o/h:

$$\frac{f_0}{f_{rs}} = 1 + \left(\frac{l_0}{h}\right)^{-1.24} \tag{5}$$

Let us note that as the equivalent shape ratio takes large values (shallower basins) the fundamental frequency predicted with Eq. (5) tends to the 1D resonance frequency. Furthermore, in Figure 7a we compare Eq. (5) with the rule to compute the normalized fundamental frequency for shear response proposed by Jiang and Kuribayashi (1988). The results of the two rules are very close.

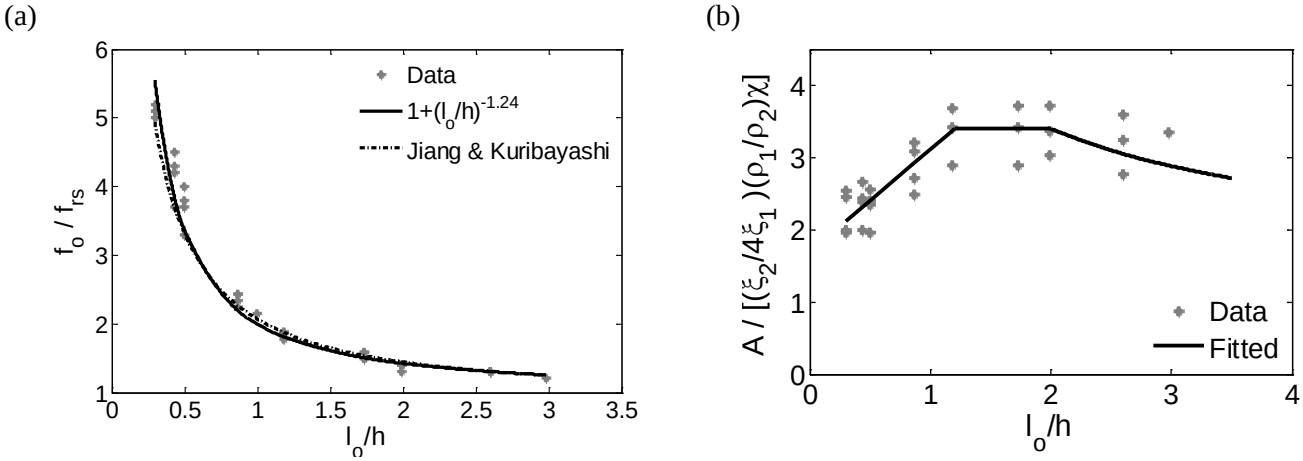

Figure 7. Proposed rule to estimate 3D amplification effects. (a) Normalized fundamental frequency f_o/f_{rs}, (b) 3D/1D amplification factor

The rule to estimate the 3D amplification factor is also in terms of the equivalent shape ratio and is normalized with the 1D elastic amplification factor $(\rho_1/\rho_2)\chi$, and the factor $\xi_2/4\xi_1$ to take into account the damping ratios, as follows:

$$\frac{A}{\tilde{\chi}} = \begin{cases} 1.7 + 1.42\left(\frac{l_0}{h}\right) & \left(\frac{l_0}{h}\right) \le 1.2 \\ 3.40 & 1.2 < \left(\frac{l_0}{h}\right) \le 2 \\ 1 + 3.64\left(\frac{l_0}{h}\right)^{-0.60} & 2 < \left(\frac{l_0}{h}\right) \end{cases} \tag{6}$$

where $\tilde{\chi} = (\xi_2/4\xi_1)\,(\rho_1/\rho_2)\chi$. As Figure 7b shows, when the equivalent aspect ratio is greater than two, the values predicted by Eq. (6) decrease, and when l_o/h approaches infinity, the 3D/1D amplification factor tends to that of the 1D elastic response times the damping relation. Equation (6) predicts values that, along with the data obtained from our simulations, are very close to the 3D/1D amplification factors computed by Olsen in [11] for

long period (0-0.5 Hz) basin response using 3D finite difference simulations. Olsen reported 3D/1D velocity amplification factors less than about 4 at the deepest parts of several southern California basins.

Finally, these rules to estimate the 3D fundamental frequency and 3D/1D amplification factor should be corrected for basin asymmetry effects. We propose the following linear rule to correct the fundamental frequency to account for such effects:

$$\frac{f_{o(asym)}}{f_{o(sym)}} = 1.36 - 0.1\left(\frac{l_o}{h}\right) \qquad \left(\frac{l_o}{h}\right) \leq 3.6 \tag{7}$$

where $f_{o(asym)}$ and $f_{o(asym)}$ are the fundamental frequencies of the asymmetric and symmetric basin, respectively. Since from our simulations we concluded that the effect of asymmetry is merely an increase of 10% in the amplification factor, the values A(sym) obtained with Eq. (6) for symmetric basins can be modified with the below equation:

$$A_{(asym)} = 1.1A_{(sym)} \tag{8}$$

to obtain the amplification factor for the asymmetric basin. With the application of formula (8), the maximum amplification factor predicted with our rules is of 3.74.

5. Conclusions

In this work we computed seismic wave amplification factors using 3D basin problems solved with the Fast Multipole Boundary Element Method. As suggested by previous studies, we found highest amplification levels for the basins with largest depth and strongest velocity ratios. However, we also explored the effects of basin asymmetry which seem to change significantly the fundamental frequency. On the contrary, the level of amplification was increased by only 10% when basin asymmetry is taken into account.

In this study we considered 5% basin damping, and we found amplification factors at the top of the basin due to incident *S*-waves to be close to four times the 1D amplification factor. We propose simple expressions to estimate the fundamental frequency and its corresponding 3D/1D amplification factor at the center of the basin. The proposed equations are expressed in terms of only the equivalent shape ratio, the basin/bedrock impedance contrast and the damping ratios of the basin and the half-space.

The results obtained in this investigation are limited to low frequencies and the small deformations that fall within the linear approximation of the basin response. Thus, to estimate amplification or de-amplification at high frequencies due to nonlinear soil response, further investigations are needed. However, simple criteria and practical rules to estimate basin amplification should be targeted in order to make the results useful for practitioners.

6. Acknowledgements

This research was financed by Electricité de France (EDF) through the MARS project (Méthodes Avancées pour le Risque Sismique).

7. References

[1] Paolucci R (1999): Shear Resonance Frequencies of Alluvial Valleys by Rayleigh's Method, *Earthquake Spectra*, **15**(3), 503-521.

[2] Rodriguez-Zuñiga JL, Sanchéz-Sesma FJ, Pérez-Rocha LE (1995): Seismic response of shallow alluvial valleys: the use of simplified models, *Bulleting of the Seismological Society of America*, **85**(3), 890-899.

[3] Papageorgiou AS, Pei D (1998): A Discrete Wavenumber Boundary Element Method for Study of the 3-D Response of 2-D Scatterers, *Earthquake Engineering and Structural Dynamics*, **27**, 619-638.

[4] Bard PY, Bouchon M (1985): The two dimensional resonance of sediment filled valleys, *Bulletin of the Seismological Society of America*, **75**, 519-541.

[5] Jiang T, Kuribayashi E. (1988): The three-dimensional resonance of axisymmetric sediment-filled valleys, *Soils and Foundations*, **28**(4), 130-146.

[6] Smerzini C, Paolucci R, Stupazzini M (2011): Comparison of 3D, 2D and 1D approaches to predict long period earthquake ground motion in the Gubbio plain, Central Italy, *Bulletin of Earthquake Engineering*, **9**(6), 2007-2029.

[7] Olsen KB, Nigbor R, Konno T (2000): 3D viscoelastic wave propagation in the upper Borrego valley, California, constrained by borehole and surface data, *Bulletin of the Seismological Society of America*, **90**(1), 134-150.

[8] Grasso E, Chaillat S, Bonnet M, Semblat JF (2012): Application of the multi-level time-harmonic fast multipole BEM to 3-D visco-elastodynamics, *Engineering Analysis with Boundary Elements*, **36**(5), 744-758.

[9] Makra K, Chávez-García FJ, Raptakis D, Pitilakis K (2005): Parametric analysis of the seismic response of a 2D sedimentary valley: Implications for code implementations of complex site effects, *Soil Dynamics & Earthquake Engineering*, **25**, 303-315.

[10] Semblat JF, Lokmane N, Driad-Lebeau L, Bonnet G. (2010): Local amplification of deep mining induced vibrations Part 2: Simulation of ground motion in a coal basin, *Soil Dynamics and Earthquake Engineering*, **30**, 947-957.

[11] Olsen KN (2000): Site Amplification in the Los Angeles Basin from Three-Dimensional Modeling of Ground Motion, *Bulletin of the Seismological Society of America*, **90**(6B), S77-S94.